Global Effects on the Variation of Ion Density and Electrostatic Potential on the Flux Surface in Helical Plasmas*)

Keiji FUJITA[1)], Shinsuke SATAKE[1,2)], Ryutaro KANNO[1,2)], Masanori NUNAMI[1,2)], Motoki NAKATA[1,2)] and José Manuel GARCÍA-REGAÑA[3)]

[1)]*Department of Fusion Science, The Graduate University for Advanced Studies, 322-6 Oroshi-cho, Toki 509-5292, Japan*
[2)]*National Institute for Fusion Science, 322-6 Oroshi-cho, Toki 509-5292, Japan*
[3)]*Laboratorio Nacional de Fusión CIEMAT, 28040 Madrid, Spain*

(Received 26 December 2018 / Accepted 22 April 2019)

Since the observation of impurity hole in LHD, which contradicts the prediction of the conventional neoclassical transport theory, several attempts have been made to explain the mechanism behind the phenomenon. Consideration of the impact of electrostatic potential variation within the flux surface, Φ_1, is one of those attempts. However, all of the numerical studies that have investigated the effect of Φ_1 to date have been conducted with local simulation codes, and no global calculation has been performed yet. Here, a global neoclassical simulation code FORTEC-3D is applied to evaluate Φ_1, including the global effects, for the first time. The global simulation result for a high-temperature low-density plasma, which corresponds to an impurity hole plasma, shows significant difference from the local simulation results in the Φ_1 profile. This indicates that consideration of the global effects is essential for quantitative evaluation of impurity neoclassical transport in an impurity hole plasma.

Keywords: neoclassical transport, impurity transport, stellarator

DOI: 10.1585/pfr.14.3403102

1. Introduction

Fusion plasmas contain a variety of ions in addition to fuel deuterium and tritium. Accumulation of such impurity ions in the plasma core leads to radiation loss or fuel dilution and decreases the performance of the plasma. Thus, understanding the behavior of impurity ions is a crucial task to realize a practical fusion reactor. Particle fluxes can be separated into two different contributions. One is turbulent flux and the other is neoclassical flux. The neoclassical part is expressed by the linear combination of driving forces:

$$\Gamma_z \equiv \left\langle \int d^3v \mathbf{v} \cdot \nabla r f_{z1} \right\rangle = -n_z \sum_a \left[D_1^{za} \left(\frac{p_a'}{p_a} + \frac{Z_a e \Phi'}{T_a} \right) + D_2^a \frac{T_a'}{T_a} \right], \quad (1)$$

where $\mathbf{v}$ is the drift velocity and f_{z1} is the first order distribution function of the impurity ion. n_a is the density of species a with charge $Z_a e$, $p_a = n_a T_a$ is the pressure, T_a is the temperature, E_r is the ambipolar electric field, the prime denotes the derivative with respect to the radial coordinate, r, and $\langle ... \rangle$ denotes the flux surface average. The coefficient D_1^{za} is positive and the ambipolar radial electric field is usually negative. In axisymmetric systems such as tokamaks, the contribution of the radial electric field term vanishes and sufficiently strong temperature gradient may drive the flux outward [1]. However, this is not usually the case for non-axisymmetric systems. Because the radial electric field term is proportional to the charge Z, it dominates the transport of high-Z ions. Thus, it has been thought that impurity accumulation is inevitable in stellarators. This prediction has been confirmed in several cases experimentally.

However, a notably exceptional phenomenon has been observed in LHD [2, 3]. It is called "impurity hole" and it represents the formation of extremely hollow density profile of the carbon impurity ions in the core region where an inwardly pointing radial electric field exists. This observation implies that the conventional neoclassical transport theory is not adequate for treating impurity transport at least in some specific parameter regions. Since then, several attempts have been made to fill the gap between the observation and the theoretical prediction. While many researchers have tried to explain the impurity hole phenomenon by investigating the turbulent contribution on the impurity transport, it has been found by a gyrokinetic simulation that the impurity turbulent flux directs inward in the impurity hole plasma [4, 5]. Improvements within the framework of neoclassical transport theory have also been a subject of research. Recent studies have shown that assumptions and approximations on which the conventional neoclassical models are constructed may be invalid for the description of impurity transport, and the inconsistency be-

author's e-mail: fujita.keiji@nifs.ac.jp

*) This article is based on the presentation at the 27th International Toki Conference (ITC27) & the 13th Asia Pacific Plasma Theory Conference (APPTC2018).

tween the observation and the conventional theoretical prediction may be, at least partially, explained by the improper simplifications [6–9].

One of the assumptions commonly employed in neoclassical transport models is that electrostatic potential is constant on each flux surface. However, it has been shown that the non-uniform part of the electrostatic potential on the flux surface, $\Phi_1 \equiv \Phi - \Phi_0(r)$, may also have significant impact on impurity transport [6]. Several studies have investigated and confirmed that the effect of Φ_1 may have substantial impact on impurity transport, and the results tend to indicate that Φ_1 acts in such a way that impurity flux is driven more inwardly rather than outwardly [10–12]. However, all the studies have been conducted with local simulation codes, and no global calculation has been performed yet. Furthermore, each study uses different approximations and the results vary accordingly as well. Among them, it has been shown that even the tangential part of the magnetic drift radically changes the profile of Φ_1 and the necessity of global calculation has been suggested [10]. Thus, we have applied a global neoclassical simulation code FORTEC-3D to evaluate Φ_1 for the first time and have compared the global result with previous local simulation results.

2. Neoclassical Transport Models

The first order guiding center distribution function is given as the solution of the following drift-kinetic equation:

$$\left(\frac{\partial}{\partial t} + \dot{\mathbf{Z}} \cdot \frac{\partial}{\partial \mathbf{Z}}\right) f_{a1} = -\dot{\mathbf{Z}} \cdot \frac{\partial}{\partial \mathbf{Z}} f_{a0} + C(f_a), \tag{2}$$

where $\mathbf{Z} = (\mathbf{X}, v_\parallel, \mu)$ are the 5-dimensional phase space coordinates and $C(f_a)$ is the linearized Fokker-Planck-Landau collision operator, respectively. $\mathbf{X}$ is the guiding center position, $v_\parallel$ is the parallel velocity and $\mu = m_a v_\perp^2/(2B)$ is the magnetic moment, where $v_\perp$ is the perpendicular component of the velocity. The lowest order guiding center distribution function is the local Maxwellian

$$f_{a0} = n_{a0}(r)\left(\frac{m_a}{2\pi T_a(r)}\right)^{3/2} \exp\left[-\frac{m_a\left(v_\parallel^2 + v_\perp^2\right)}{2T_a(r)}\right]. \tag{3}$$

When the electromagnetic potentials are static, the time derivatives of the guiding center variables are given as

$$\dot{\mathbf{X}} = \frac{\mathbf{B}^*}{B_\parallel^*} v_\parallel + \frac{1}{eB_\parallel^*}\mathbf{b} \times (\mu \nabla B + Ze\nabla\Phi), \tag{4}$$

$$\dot{v}_\parallel = -\frac{1}{mv_\parallel}\dot{\mathbf{X}} \cdot (\mu \nabla B + Ze\nabla\Phi), \tag{5}$$

$$\dot{\mu} = 0, \tag{6}$$

where $\mathbf{b} = \mathbf{B}/B$, $\mathbf{B}^* = \nabla \times \mathbf{A}^*$ is corrected magnetic field with the guiding center vector potential $\mathbf{A}^* = \mathbf{A} + mv_\parallel \mathbf{b}/e$ and $B_\parallel^* = \mathbf{B}^* \cdot \mathbf{b}$. The equations of motion are derived in such a way that the conservation of the phase space volume is ensured [13].

Neglecting the correction term in $B_\parallel^*$ and using low-beta approximation ($\nabla \times \mathbf{b} \simeq \mathbf{B} \times \nabla B/B^2$) yields another set of equations:

$$\dot{\mathbf{X}} = v_\parallel \mathbf{b} + \mathbf{v}_m + \mathbf{v}_E, \tag{7}$$

$$\dot{v}_\parallel = -\frac{1}{mv_\parallel}\dot{\mathbf{X}} \cdot (\mu \nabla B + Ze\nabla\Phi), \tag{8}$$

$$\dot{\mu} = 0, \tag{9}$$

where $\mathbf{v}_m = (1/Ze)(mv_\parallel^2 + \mu B)\mathbf{B} \times \nabla B/B^3$ and $\mathbf{v}_E = \mathbf{B} \times \nabla\Phi/B^2$. Furthermore, removing the radial component of the guiding center velocity in the left-hand side of (2) reduces the dimension of the phase space from five to four and allows us to solve the equations on each flux surface independently. This is called radially-local approximation and models based on this approximations are called "local" models. The most common way to do this is by dropping the magnetic drift term $\mathbf{v}_m$ entirely and the radial component of the $E\times B$ drift, $\mathbf{v}_E$, from (7). The resulting equations are

$$\dot{\mathbf{X}} = v_\parallel \mathbf{b} + \mathbf{v}_{E0}, \tag{10}$$

$$\dot{v}_\parallel = -\frac{1}{mv_\parallel}(v_\parallel \mathbf{b} + \mathbf{v}_m + \mathbf{v}_{E0}) \cdot (\mu \nabla B + e\nabla\Phi), \tag{11}$$

$$\dot{\mu} = 0, \tag{12}$$

where $\mathbf{v}_{E0} = \mathbf{B} \times \nabla\Phi_0(r)/B^2$. These types of local models have been almost exclusively used for neoclassical simulations. Still, keeping the radially-local approximation, we can retain the effect of the magnetic drift partially. The local models which retain the components of the magnetic drift tangential to the flux surface ($\hat{\mathbf{v}}_m \equiv \mathbf{v}_m - (\mathbf{v}_m \cdot \nabla r)\mathbf{e}_r$) in (7) are called zero orbit width (ZOW) models. It has been shown that even the tangential part of the magnetic drift changes the dependence of the neoclassical transport on the radial electric field, especially when the radial electric field is weak [14]. Approximating the collision operator in (2) by the pitch-angle scattering operator enables us to treat the magnitude of velocity v as a parameter and reduce another dimension of the phase space. This is called mono-energetic approximation. In addition to the 5-dimensional global model with the full linearized Fokker-Planck-Landau operator, FORTEC-3D is also able to solve those local models.

Before proceeding to the next section, let us briefly discuss the primary reason why Φ_1 may not be negligible for impurity transport analysis. Look at the equation for parallel acceleration (5) or (8). The leading terms in those equations are parallel gradient of magnetic field $\nabla_\parallel B$ and electrostatic potential $\nabla_\parallel \Phi$, where $\nabla_\parallel \equiv \mathbf{b} \cdot \nabla$. The latter is usually not taken into account since Φ is assumed to be a flux function, i.e., Φ_1 does not have the flux surface component. The ratio of the magnitude of the two terms is

$$\frac{Ze\nabla_\parallel \Phi}{\mu \nabla_\parallel B} \sim \frac{Ze\Phi_1}{T\Delta B}, \tag{13}$$

where ΔB represents the typical depth of the magnetic well. $e\Phi_1/T$ is the order of $10^{-3} \sim 10^{-1}$. Thus, it is reasonable to neglect the Φ_1 term for bulk species. However, the ratio may approach to or exceed the order of unity for impurity ions due to their high Z number. Then, the particle trapping behavior is changed by Φ_1, and so is the diffusion process. A similar argument can be applied to the ratio between the radial $E \times B$ drift generated by Φ_1 and the magnetic drift:

$$\frac{v_{E1}}{v_m} \sim \frac{Ze\Phi_1}{T}\frac{R}{a}, \tag{14}$$

where R is the major radius of the device and a is the minor radius of the plasma, although the effects of those radial drifts in the orbit equations cannot be considered in local simulations.

3. Evaluation of Φ_1

Here we consider a hydrogen plasma ($Z_i = 1$) which contains only single impurity species and suppose the impurity ion is in thermal equilibrium with the bulk ion: $T_z = T_i$. Then imposing the quasi-neutrality condition, $\sum_a Z_a n_a = 0$, on the density up to the first order

$$n_a = n_{a0} \exp\left(-Z_a e\Phi_1/T_a\right) + n_{a1}, \tag{15}$$

yields the expression

$$-e^2\Phi_1\left(\frac{n_{i0}}{T_i} + \frac{n_{e0}}{T_e} + Z_z^2\frac{n_{z0}}{T_i}\right) + e\left(n_{i1} - n_{e1} + Z_z n_{z1}\right) = 0. \tag{16}$$

Here, $Z_a e\Phi_1/T_a \ll 1$ is assumed for all species. Assuming the electron response is adiabatic ($n_{e1} = 0$) and the concentration of the impurity is negligibly low ($Z_z n_z \simeq 0$), the equation for Φ_1 is reduced to

$$\Phi_1 = \frac{1}{en_0}\left(\frac{1}{T_i} + \frac{1}{T_e}\right)^{-1} n_{i1} = \frac{1}{en_0}\left(\frac{1}{T_i} + \frac{1}{T_e}\right)^{-1}\int d^3v f_{i1}, \tag{17}$$

where $n_0 = n_{i0} \simeq n_{e0}$. This expression is used in several studies to compute Φ_1 (e.g., [10, 11, 15]). Some assumptions in the argument above may be questionable, and models based on more relaxed assumptions have also been investigated [12, 16]. Yet, the primary purpose of this study is not to make an accurate computation of Φ_1 but to see if and how the global effects make a difference compared with local results. Thus, we adopt the simplified expression (17) in this study to assess Φ_1. This means that the distribution of Φ_1 computed in this study is essentially the spatial distribution of f_{i1}, which is the solution of the drift-kinetic equation (2) for the bulk ion. However, it should be noted that the effect of Φ_1 is not considered in the calculation of f_{i1}, since the Φ_1-effect is assumed to be small for $Z = 1$ hydrogen.

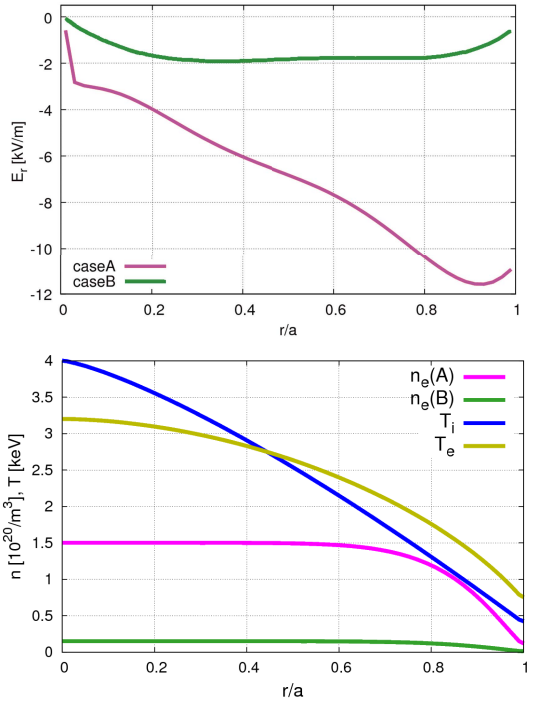

Fig. 1 Plasma profiles for case A and B. In the top, the magenta line represents E_r profile for A and the green line for B. In the bottom, the temperature and density profiles are plotted.

We have considered two different LHD plasmas (Fig. 1): while plasma A corresponds to a standard ion root plasma, plasma B, of which density is ten times lower than that of plasma A, is closer to an impurity hole plasma. The profiles of those plasmas correspond to the plasma A and B in reference [10], respectively, which investigated the effect of the tangential magnetic drift on Φ_1 given by (17) using the codes EUTERPE and KNOSOS. The study showed that the profile of Φ_1 was largely modified by the inclusion of the tangential magnetic drift. While the amplitude was increased by a factor of around 2 for case A and case B both, the change in the phase was more distinctive for case B. The relative position of positive and negative peaks are inverted, and stellarator symmetry, seen in the result without the magnetic drift, was lost in the case with the tangential magnetic drift (see Fig. 2). Stellarator symmetry is the invariance under the transformation $(\theta, \zeta) \to (-\theta, -\zeta)$, and as it can be seen in Fig. 3, the magnetic field in LHD has this property. We will see if these features are reproduced by FORTEC-3D, and if and how the global effects change the result further. Nevertheless, it should be noted that KNOSOS solves drift-kinetic equation only for trapped particles, and the equation is based on an approximation in which the magnetic field configuration is close to ominigeneity. As the authors note, however, results based on this approximation may be qualitatively inaccurate especially for $r/a < 0.5$. Thus we make a comparison here to see the qualitative tendency in how the

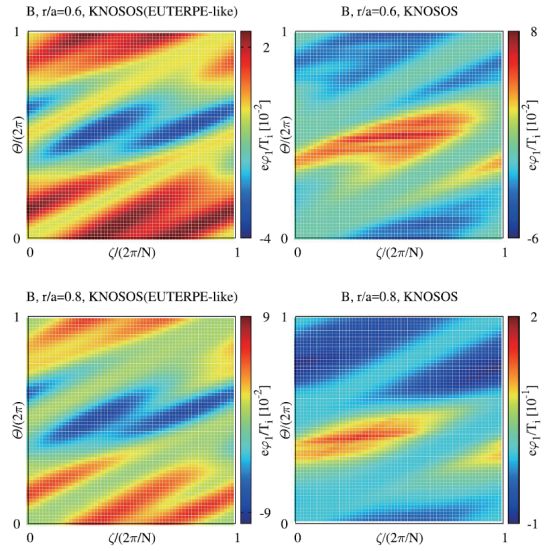

Fig. 2 Figure 9 in [10]. $e\Phi_1/T_i$ calculated by KNOSOS with (right) and without (left) the tangential magnetic drift at $r/a = 0.6$ (top) and 0.8 (bottom) for an impurity hole plasma.

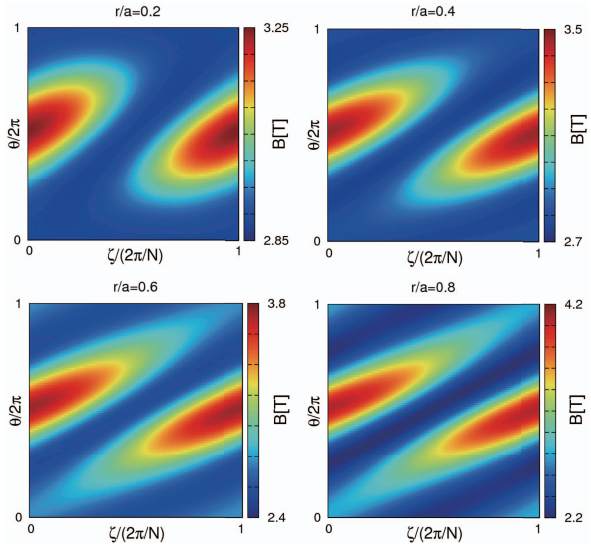

Fig. 3 Magnetic field strength at $r/a = 0.2,\ 0.4,\ 0.6$, and 0.8 in LHD.

magnetic drift changes the profile of Φ_1, focusing on their results for $r/a > 0.5$.

4. Numerical Results

In this section, we discuss the numerical results we have obtained. For each case in this study, we calculated Φ_1 using three different models: (I) the standard local model which entirely ignores the magnetic drift $\mathbf{v}_m$; (II) ZOW model which includes the tangential magnetic drift $\hat{\mathbf{v}}_m$; and (III) global model which retains the full magnetic drift. In Fig. 4, $e\Phi_1/T_i$ for case A is mapped on θ-ζ plane, where θ and ζ are poloidal and toroidal angle in Boozer coordinate system, respectively. From the top, each row corresponds to $r/a = 0.2, 0.4, 0.6$, and 0.8, respectively. The leftmost column is the result of the model (I) calculated with EUTERPE in [10]. The next from the leftmost column is the result of the same model obtained with the local version of FORTEC-3D. They show good agreement on each flux surface. The third from the left is the ZOW result calculated with the local version of FORTEC-3D. The modification due to the tangential magnetic drift is small in the inner half region ($r/a = 0.2$ and 0.4). Although the impact of the tangential magnetic drift is more visible in the outer half region ($r/a = 0.6$ and 0.8), the relative position of positive and negative regions are not largely shifted. Finally, the rightmost column is the result of the global model (III) calculated with FORTEC-3D. While the effect of the magnetic drift is mild in the inner half region, the impact becomes more appreciable in the outer half region. Still, comparing the results with the standard local results, the modification are continuous and no radical changes such as phase inversion are found.

In contrast to case A, a notable change due to the global effects was found for case B. Figure 5 shows the profile of Φ_1 for case B. As for case A, the first and second columns from the left are results of the model (I) calculated with EUTERPE and FORTEC-3D, respectively, and they show reasonable agreement. In the result of this model, the phase of Φ_1 is almost stellarator symmetric. This is a consequence expected from the property of the local drift-kinetic equation in the collisionless limit [15]. Note that this feature is not generally shared in the result of the same model for case A, where the collision frequency is higher than this case. It can be noted that once the tangential magnetic drift is included, the phase of Φ_1 is completely changed: the relative position of the positive and negative regions are largely shifted. The way of the modification in the phase of Φ_1 at $r/a > 0.5$ is somewhat similar to that in Fig. 2. However, no consistent tendency in the effects on the amplitude is found. Finally, in the global result, the way of the modification is similar to that in the ZOW result, but some differences are found as well. The global result shows smaller amplitude of Φ_1 than the ZOW result, especially at $r/a > 0.5$. Further, while both the ZOW result and the global result mainly consist of stellarator symmetric components, the Fourier composition of the global result is, although the sign is opposite, closer to that of the standard local result than the ZOW result is.

In an LHD plasma, the sign of the tangential component of the magnetic drift $\hat{\mathbf{v}}_m$ is, on average, opposite to that of the $E \times B$ drift, $\mathbf{v}_{E0}$, generated by the negative ambipolar electric field. When the absolute value of the electric field is large, as for case A, the effect of $\hat{\mathbf{v}}_m$ is negligible relative to the effect of $\mathbf{v}_{E0}$. However, when the amplitude of the electric field is small, $\hat{\mathbf{v}}_m$ becomes of the same order as $\mathbf{v}_{E0}$, and can even be larger. Then the direction of the guiding center drift on the flux surface is inverted and, accordingly, so is the phase of Φ_1. This seems to be the

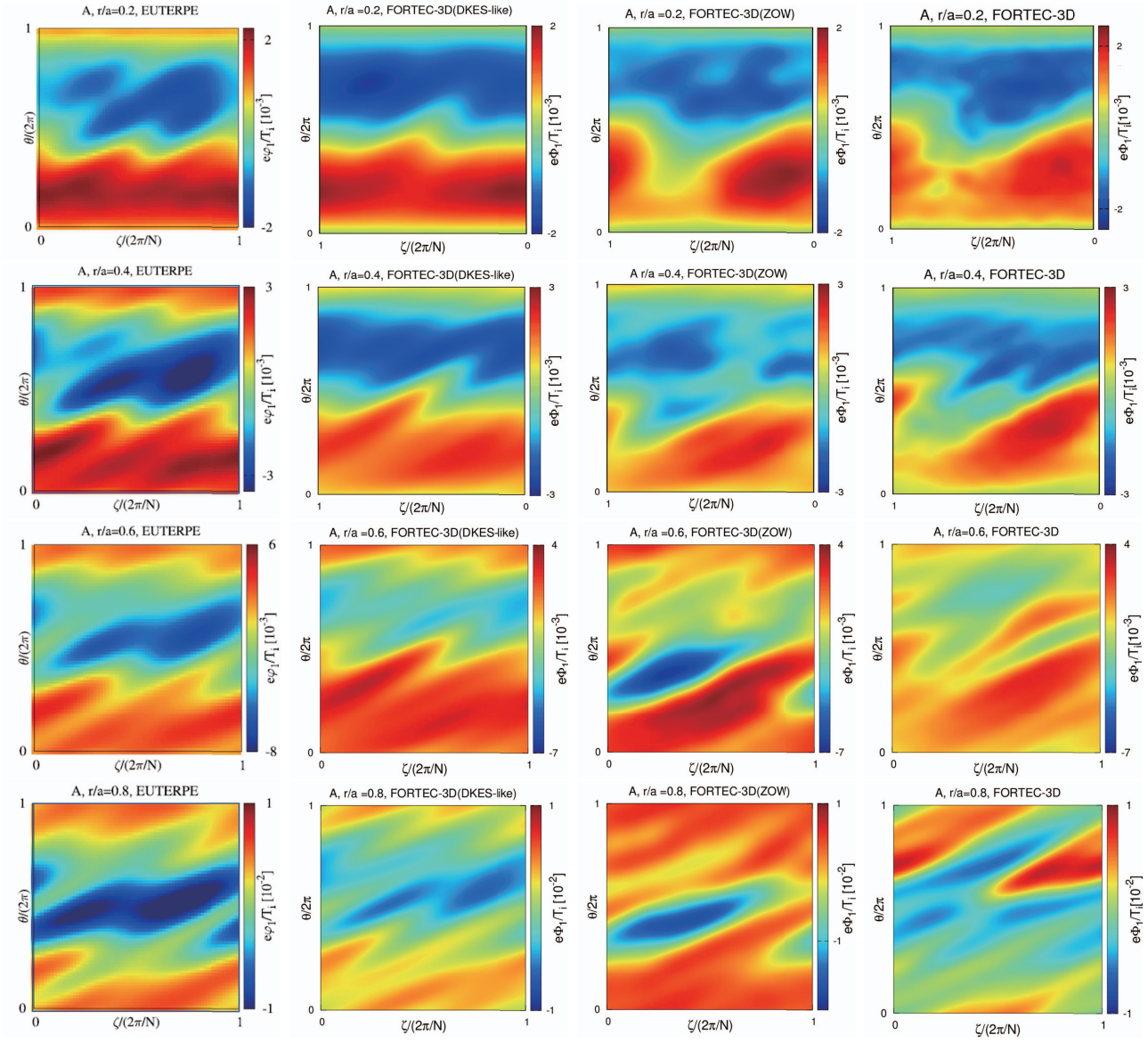

Fig. 4 $e\Phi_1/T_i$ mapped on θ-ζ plane in Boozer coordinate system. The left two columns are results of the standard local model (I) calculated with EUTERPE in [10] and local version of FORTEC-3D, respectively. The right two columns are results of ZOW (II) and global model (III), respectively. Note that not all color scales are the same.

primary reason that the phase inversion was seen in case B but not in case A. Further, different phases of Φ_1 were produced by the ZOW model and the global model, respectively. This means the inclusion (or the lack of) the radial component of the magnetic drift in the model changes the Fourier composition of Φ_1. This difference may be crucial since the mode composition determines how the $E\times B$ drift due to Φ_1 couples to f_{z1} in generating the radial particle flux. Although we cannot explain how these differences result in impact on the radial impurity flux without performing computation, significant difference in Φ_1 is indeed found between the results of global and local simulations.

5. Conclusion

In this article, we have investigated the global effects on Φ_1 in a condition similar to an impurity hole plasma, and significant difference in the profile of Φ_1, which is calculated from the ion density variation, was found between local and global neoclassical calculations. This implies that the finite orbit effects become non-negligible in impurity hole plasmas where the collisionality is lower and the $E \times B$ drift is weaker than those in standard ion root plasmas. This suggests that the global drift-kinetic model is essentially required to evaluate Φ_1 potential profile and that the amplitude and direction of radial impurity flux in global simulations may also be significantly different from those in local simulations. The difference may come not only from the difference in Φ_1, but also from the difference in the first order distribution function of the impurity given as the solution of the global drift-kinetic equation. Nevertheless, the inversion of the phase of Φ_1 does not nec-

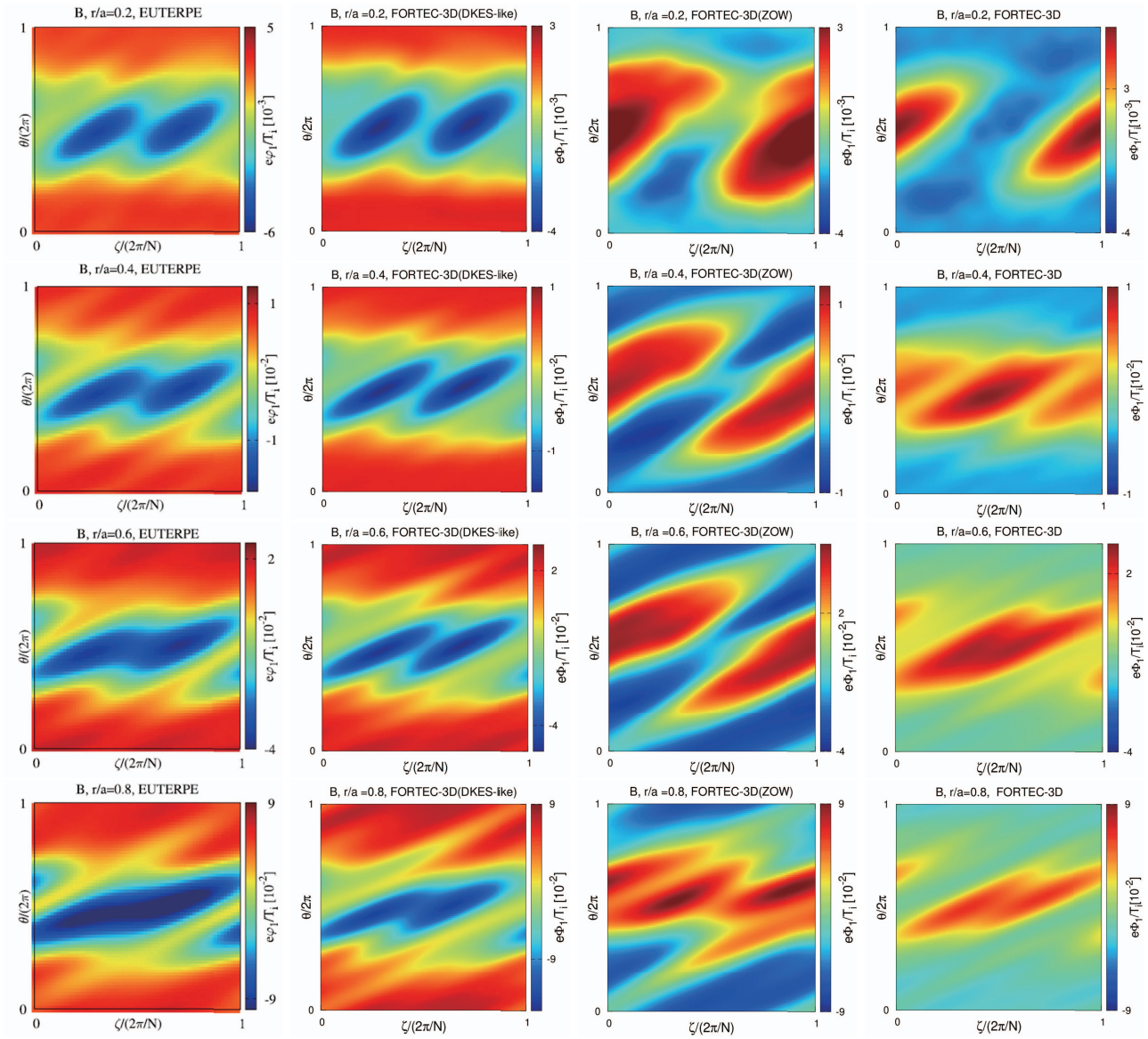

Fig. 5 $e\Phi_1/T_i$ mapped on θ-ζ plane in Boozer coordinate system. The left two columns are results of the standard local model (I) calculated with EUTERPE in [10] and local version of FORTEC-3D, respectively. The right two columns are results of ZOW (II) and global model (III), respectively. Note that not all color scales are the same.

essarily mean the inversion of the direction the effects of Φ_1 act on impurity flux, since the distribution of the impurity ion may also be modified in such a way that the effect caused by the difference is canceled. Assessment of the accuracy of numerical evaluation of Φ_1 is also important for investigating its impact in real plasmas. In addition to the global simulation of impurity transport in LHD including Φ_1, comparisons between numerical simulation results and available experimental data on Φ_1 profile, such as the radial electric field due to Φ_1 in the TJ-II [16], will be presented in our future publications.

Acknowledgments

The authors would like to thank Dr. J.L. Velasco in CIEMAT for providing the reference data. This work is performed under the auspices of the NIFS Collaborative Research Program, No. NIFS18KNST132 and NIFS16KNXN315. This work is also supported in part by JSPS KAKENHI Grant No. 18H01202.

[1] S.P. Hirshman, Phys. Fluids **19**, 155 (1976).
[2] K. Ida *et al.*, Phys. Plasmas **16**, 056111 (2009).
[3] M. Yoshinuma *et al.*, Nucl. Fusion **49**, 062002 (2009).
[4] M. Nunami *et al.*, 26th IAEA FEC, TH/P2-3 (2016).
[5] M. Nunami *et al.*, 27th IAEA FEC, TH/P6-8 (2018).
[6] J.M. García-Regaña *et al.*, Plasma Phys. Control. Fusion **55**, 074008 (2013).
[7] P. Helander *et al.*, Phys. Rev. Lett. **118**, 155002 (2017).
[8] S. Newton *et al.*, J. Plasma Phys. **83**, 905830505 (2017).
[9] J.L. Velasco *et al.*, Nucl. Fusion **57**, 016016 (2016).
[10] J.L. Velasco *et al.*, Plasma Phys. Control. Fusion **60**, 074004 (2018).

[11] J.M. García-Regaña *et al.*, Nucl. Fusion **57**, 056004 (2017).
[12] A. Mollén *et al.*, Plasma Phys. Control. Fusion **60**, 084001 (2018).
[13] R.G. Littlejohn, J. Plasma Phys. **29**, 111 (1983).
[14] S. Matsuoka *et al.*, Phys. Plasmas **22**, 072511 (2015).
[15] I. Calvo *et al.*, Plasma Phys. **84**, 905840407 (2018).
[16] J.M. García-Regaña *et al.*, Plasma Phys. Control. Fusion **60**, 104002 (2018).